journal

J. Am. Ceram. Soc., 89 [6] 1890–1896 (2006)
DOI: 10.1111/j.1551-2916.2006.01045.x

Rheological Behavior and Slip Casting of Al_2O_3–Ni Aqueous Suspensions

A. Javier Sánchez-Herencia, Nicolás Hernández, and Rodrigo Moreno†

Instituto de Cerámica y Vidrio, CSIC, Campus de Cantoblanco, Madrid E-28049, Spain

A strong effort has been devoted recently toward processing of metal–ceramic composites with tailored microstructure by colloidal methods. The aim of this work is to optimize the rheological behavior of concentrated Al_2O_3–nickel (Ni) aqueous suspensions and further slip casting in order to obtain dense green composites. Compositions with Ni relative contents ranging from 5 to 75 vol% were prepared from suspensions with high solids loadings (50 vol%) by adjusting the colloidal stability of each component in terms of pH, mobility, dissolution conditions, and influence of polyelectrolytes. The rheological properties were measured under controlled rate and controlled stress conditions at different basic pH conditions and contents of polyelectrolyte. Better rheological conditions of the mixtures were found for pH 10 and 1.0 wt% polyelectrolyte. Minimum viscosity was obtained for suspensions containing 15 vol% of Ni. The analysis of flow curves demonstrates that the suspensions form a structure at very low shear, hindering sedimentation. Homogeneous slip cast bodies with green densities up to 70% of theoretical and up to 75 vol% Ni were sintered in Ar to achieve dense biphasic composites.

I. Introduction

Nickel (Ni) and Ni-matrix composites have received increased attention because of their potential as either functional or structural applications, such as electrodes for fuel cells and thermal barrier coatings, respectively.[1,2]

From a structural point of view, the introduction of a ductile phase into a brittle ceramic matrix is a suitable mechanism for reinforcing the mechanical response of the matrix. A variety of ceramic–metal composites have been studied, with the aluminum oxide (Al_2O_3)–Ni system being one of the most extensively studied.[3–5] In this sense, several variables have been related to the reinforcement, including composition,[6] inclusion shape [7] and size,[8] and sintering conditions.[9] The inclusion of a ductile phase into a rigid alumina matrix improves the mechanical behavior through crack deflection, microcrack toughening, crack bridging, and crack blunting.

To achieve an efficient reinforcement, a high level of dispersion of the secondary phase into the matrix is required, in addition to achieving a high relative density. For this reason, pressure-sintering techniques have been preferred for the manufacture of Al_2O_3–Ni composites. However, some effort has been made for manufacturing these materials by pressureless sintering using powder forming routes, such as extrusion, die pressing, or injection molding.[9,10] Also, tape casting and lamination have been used to reinforce alumina matrices by intercalating metal and ceramic layers.[11] The control in the processing and sintering conditions opens the possibility of designing graded structures.[12]

The colloidal approach has been well demonstrated to be a useful way to obtain dense ceramics with high microstructural uniformity, reliability, and complexity.[13–16] Colloidal forming methods have been also used for metals and cermets,[17,18] but a deep characterization of the suspensions is much less frequent because of the high density of the metal powders and their complex surface behavior in water.

The shape forming of non-aqueous Ni suspensions has been reported elsewhere,[19,20] but the characterization of the rheological properties has not received due attention. Tseng[21–23] studied the rheological behavior of non-aqueous Ni suspensions dispersed with polymeric surfactants. These suspensions exhibited a shear-thinning behavior that suggested the formation of a flocculated structure that broke down on shearing. The aggregation state was characterized by a fractal dimension (D_f), which is estimated from the measured values of the yield stress.[23,24]

Previous work has demonstrated that Ni powders can be processed by colloidal forming methods in water if the surface properties are carefully controlled.[25,26] The maximum stability of Ni powders (with a mean size of 2.5 μm) in water was found for suspensions dispersed with an acrylic-based polyelectrolyte and basic pH (~10), where the particle surfaces become NiO enriched and surface dissolution is prevented. The rheological behavior of concentrated suspensions of this Ni has also been studied. Suspensions with solids loadings up to 40 vol% were prepared, and green densities of 53% of the theoretical were obtained.

One of us has studied previously the rheological behavior of aqueous suspensions of the same alumina powder used herein.[27] Better dispersion was achieved for the polyelectrolyte type and content we have used now. However, these suspensions had a natural pH by 9, at which Ni exhibits a large viscosity and thixotropy. As the Ni particles form a strong structure and govern the rheology, suspensions of alumina must be prepared at the optimum pH for Ni in order to avoid undesired pH variations. Hence, the rheology of alumina is studied for the different solids loadings at pH 9 (natural pH), 10, and 11.

This work deals with the preparation of concentrated suspensions of Al_2O_3–Ni mixtures, and the study and optimization of their rheological behavior. The stability of the suspensions of the pure components and the mixtures was studied considering the ξ potential values and the effect of dispersing agents, pH modification, and solids loading on the rheology. Rheological models were used to predict the maximum packing fraction of the suspensions. The suspensions were slip cast on plaster molds to obtain green bodies with relative densities up to 70% of the theoretical.

II. Experimental Procedure

The following powders were studied: a commercial Ni powder (INCO T-110, Mississauga, ON, Canada) with a mean particle size of 2.5 μm, a surface area of 1 m^2/g and a density of 8.813 g/cm^3, and a high-purity α-Al_2O_3 (CONDEA HPA05, Tucson,

G. Messing—contributing editor

Manuscript No. 21423. Received January 24, 2006; approved February 27, 2006.
Presented at the 9th International Ceramic Processing Science Symposium, Coral Springs, FL, January 8–11, 2006.
This work has been supported by CICYT (Spain) under contract MAT2003-00836.
†Author to whom correspondence should be addressed. e-mail: rmoreno@icv.csic.es

AZ) with a mean particle size of 0.35 μm, a surface area of 9.5 m^2/g, and a density of 3.98 g/cm^3.

According to previous studies,[25,26] concentrated aqueous suspensions of Ni powders were prepared with a polyelectrolyte at basic pH in order to prevent dissolution and to promote the development of NiO-enriched species at the surface. An acrylic-based polyelectrolyte (Duramax D-3005, Rohm & Haas, Philadelphia, PA, Mw ~2400) was used as a dispersant at a concentration of 1 wt% on a dry-solids basis. pH adjustments were made by adding tetramethylammonium hydroxide (TMAH) up to pH values of 9, 10, and 11. Ni suspensions with volume fraction of solids (ϕ) ranging from 0.15 to 0.40 (60–85.2 wt%, respectively) were prepared.

Alumina aqueous suspensions were prepared to volume fraction of solids ranging from 0.37 to 0.55 (70–87 wt%) by dispersing with 0.8 wt% (on a dry-solids basis) of the same deflocculant used for Ni powders. In order to avoid undesired variations of pH in the mixtures, rheological studies for alumina suspensions were performed at pH values of 9, 10, and 11, as well. As in the previous case, pH adjustments were made by adding TMAH.

Suspensions of mixtures of Ni and Al_2O_3 were prepared always to a total volume fraction of solids of 0.5. Mixtures were prepared to relative ratios of Ni of 5, 10, 15, 25, 50, and 75 vol%, thus covering both Al_2O_3-rich and Ni-rich regions. These mixtures were dispersed with 1.0 wt% polyelectrolyte and pH 10.

All suspensions were prepared in deionized water using an ultrasound probe (IKA 400S, IKA, Staufen, Germany) for 1 min and maintained for 24 h under mechanical stirring.

To characterize the stability of suspensions dispersed with a polyelectrolyte at basic pH, ξ potential measurements were performed on diluted suspensions using the microelectrophoresis technique (Zeta-meter 3.0^+, Zetameter, Staunton, VA). The ionic strength was fixed with $10^{-3}M$ KCl.

Rheological characterization was carried out using a rheometer RS50 (Haake, Karlsruhe, Germany) with a double-cone/plate sensor configuration (DC60/2°, Haake) that requires a sample volume of 5 mL. Temperature was maintained constant at 25±0.5°C. The flow behavior was measured by two different testing modes: controlled shear (CR) and controlled stress (CS). To obtain the high shear flow behavior CR experiments were carried out using a measuring program in three stages: first, a linear increase of shear rate; a plateau at the maximum shear rate for 1 min; and decrease to zero. The characterization at the low shear rate region was performed through CS experiments. In these measurements, shear stress is linearly increased until viscous flow occurs. For simplicity in the flow curves only the up-ramps have been plotted. The rheological behavior of the slurries was fit to regression models having two and four parameters. Slips were prepared at different solids loadings and the variation of viscosity versus volume fraction of solids was used to predict the maximum packing fraction (ϕ_m) before the suspension behaved as a solid. To do so, the behavior at extreme shear regions must be well differentiated. For this purpose, the curves were fitted to the Cross model: Eq. (1)

$$\frac{\eta_0 - \eta}{\eta - \eta_\infty} = (k\dot{\gamma})^m \tag{1}$$

where η_0 is the extrapolation of the viscosity to the zero shear rate and is referred to as zero shear viscosity, η_∞ is the limit viscosity, which refers to that extrapolated to infinite shear rate, $\dot{\gamma}$ is the shear rate, k is a constant with dimensions of time, and m is a dimensionless constant. In this work, η_0 was obtained by extrapolating to zero shear the values measured in CS mode, while CR curves were used to obtain η_∞ values. The variation of the limit viscosity (η_∞) as a function of volume fraction of particle was studied considering the Krieger–Dougherty model in order to predict the maximum solids loading to which the slips maintain stable Eq. (2):

$$\eta = \eta_s(1 - \phi/\phi_m)^{-[\eta]\phi_m} \tag{2}$$

which allows the calculation of the maximum packing fraction, considered as the volume fraction of solids where the viscosity tends to infinity. In this equation, η_s is the viscosity of the dispersing medium and [η] is the intrinsic viscosity, which has a value of 2.5 for spherical particles and increases as sphericity decreases. Then the modified Krieger–Dougherty model can be used in which the exponent $[\eta].\phi_m$ is replaced by a coefficient n.

Suspensions of pure Ni, pure Al_2O_3, and their mixtures were slip cast on plaster of Paris molds to obtain disks and plates. As-cast samples were dried in air for 24 h. Green densities were determined by the Archimedes method in mercury.

Samples were sintered at 1450°C for 2 h with heating and cooling rates of $5°C \cdot min^{-1}$ under a flowing atmosphere of Argon with 1 vol% of oxygen. This atmosphere has been used to force the formation of $NiAl_2O_4$ spinel on the outside surfaces of the samples that helps in further polishing processes[28,29]. Sample surfaces were ground to remove the outer oxidation shell before density measurements. Sintered densities were determined by the Archimedes method in water. Scanning electron microscopy (SEM, Carl Zeiss, DSM-950, Germany) observations were made on fractured green samples as well as polished sintered ones. Chemical etching was performed by dipping the polished samples into a 50/50 solution of acetic acid/nitric acid for 5 s.

III. Results and Discussion

(1) Rheological Behavior of Monophase Suspensions

The complex surface behavior of Ni powders in water has been reported elsewhere.[13] Under acidic conditions, Ni^{2+} species prevail. The isoelectric point was found to occur at pH 3.5–4, but the ξ potential showed a constant value at pH ranging from 4 to 9, which was assigned to the existence of NiO(OH) species. Powders treated under basic conditions (pH >9) led to NiO-enriched surfaces.

The surface behavior of Al_2O_3 aqueous slurries has been widely reported in the literature, the isoelectric point occurring at pH = 9, although the adsorption of an acrylic polyelectrolyte causes the isoelectric point to shift toward lower pH.

Figure 1 shows the variation of ξ potential with polyelectrolyte content for suspensions of either Ni or Al_2O_3 prepared at their natural pH (pH 8.5 and 9, respectively, without any pH adjustment). Maximum values of ξ potential of −40 and −60 mV are reached for Ni and Al_2O_3, respectively, thus demonstrating the high stability of both powders under these dispersing conditions.

The rheological behavior of Ni slips with a volume fraction of solids of 0.35 is shown in Fig. 2, where the CR flow curves of slips prepared at the different pHs are plotted. A minimum of

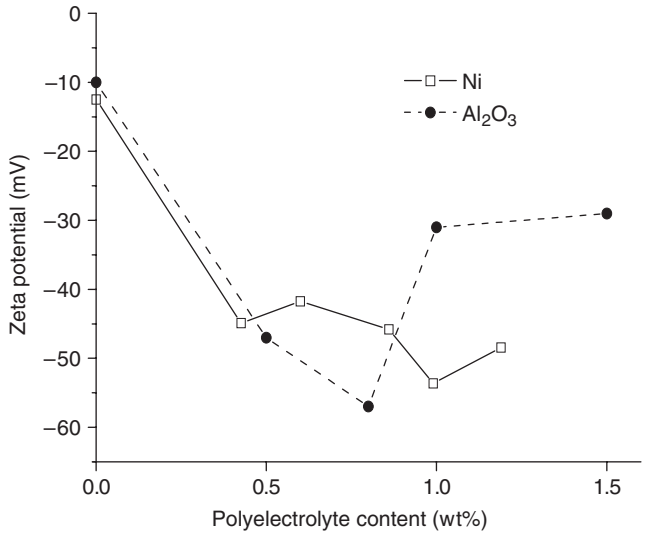

Fig. 1. ξ potential values of aluminum oxide and nickel powders in water with different amounts of dispersant at their natural pH (~9).

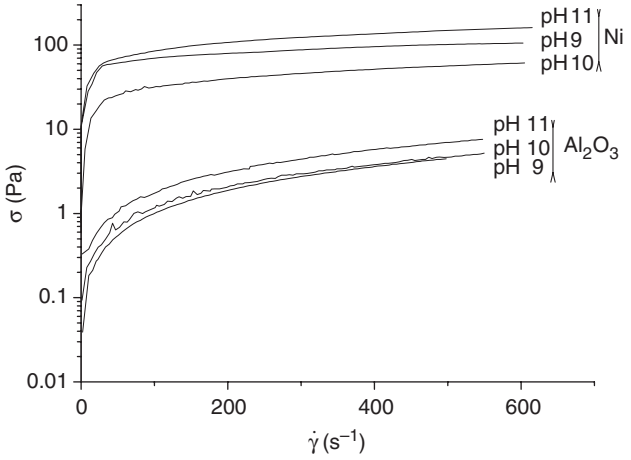

Fig. 2. Flow curves of nickel and aluminum oxide suspensions with volume fractions of 0.35 and 0.37, respectively, measured in controlled shear mode at pH 9, 10, and 11. Only up-curves are shown.

viscosity is reached for suspensions prepared at pH 10. This can be explained considering that pH 9 is very close to the equilibrium pH and there is still a considerable amount of hydroxylated species. At pH 11, the concentration of base necessary to reach this high pH is very large and the increased concentration of counter ions in the liquid medium leads to a double-layer thinning effect. Figure 2 also plots the CR flow curves of Al_2O_3 suspensions prepared to a similar volume fraction of particles (0.37) and the same pH values considered for Ni suspensions. The minimum viscosity is reached at the natural pH, while the addition of TMAH to increase the pH has a deleterious effect on viscosity. However, the viscosity of Ni suspensions is much higher than that of alumina suspensions, so the composite rheology should be governed by Ni. The increase in viscosity of alumina when pH changes from 9 to 10 is negligible as compared with the variation of Ni viscosity when the pH is changed. Similar observations were obtained for the slips prepared with other solids loadings. Accordingly, the homogeneity of the mixtures will be improved if pH 10 is maintained for the optimum dispersant content.

Figure 3 shows the flow curves measured in CR mode for the Ni suspensions prepared at different volume fraction of solids and a constant pH of 10. As expected, the rheological behavior becomes more complex as solids loading increases, the flow behavior changing from nearly Newtonian for lower concentrations to very shear thinning for the more concentrated suspensions. This suggests the formation of some structure in

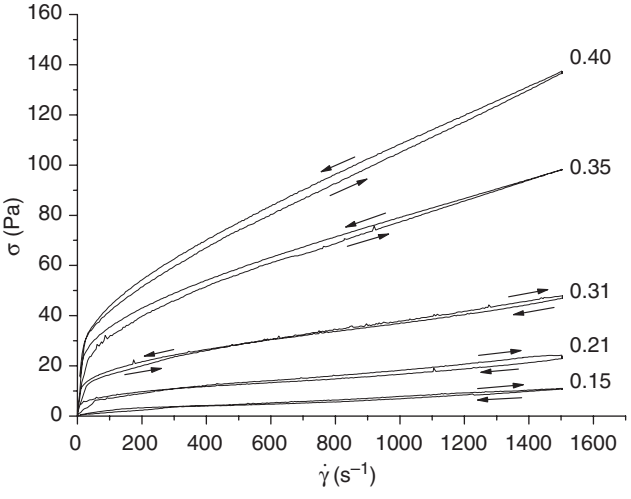

Fig. 3. Flow curves of nickel suspensions with different volume fractions measured in controlled shear mode (1 wt% polyelectrolyte and pH 10).

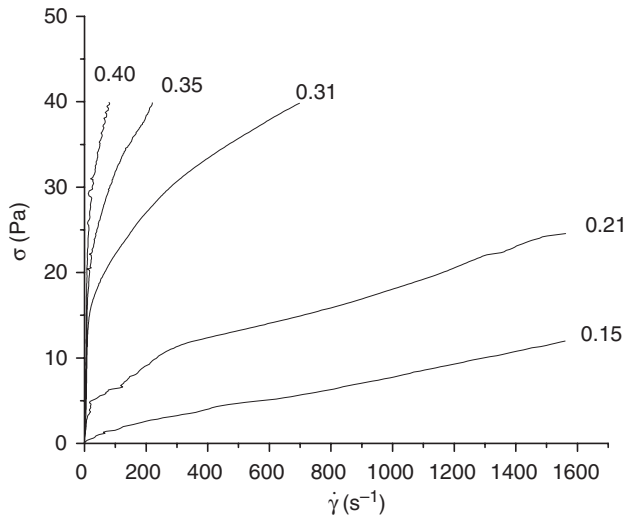

Fig. 4. Flow curves of nickel suspensions with different volume fractions measured in controlled stress mode (1 wt% polyelectrolyte and pH 10). Only up-curves are shown.

the low shear region and some time dependency is observed in the flow curves. The flow curves obtained for the same suspensions measured at CS conditions are shown in Fig. 4.

Similarly, Figs. 5 and 6 plots the flow curves of alumina suspensions prepared at pH 10 and different volume fractions of solids, measured at CR and CS conditions, respectively. The less concentrated suspension ($\phi = 0.37$) has a very low viscosity and a slight shear thickening behavior. When solids loading increases, the suspension shows a shear thinning behavior. Alumina suspensions with low viscosity can be prepared to solids loadings up to 55 vol%, while very high viscosities are obtained for Ni above a volume fraction of 0.40.

From these flow curves, the extrapolated values of viscosity were plotted against the volume fraction of particles. It was observed that η_0 values were several orders of magnitude higher than the corresponding η_∞ values. That is, there are strong differences between the flow behavior at very low shear rates and very high shear rates. Suspensions behave as shear thinning fluids, with a strong structure that must be broken for the flow to occur. This very shear thinning behavior leads to very large errors in η_0, so that fitting to the Krieger–Dougherty model to predict the maximum packing fraction was performed only for η_∞ values obtained from the CR curves. Figure 7 shows the variation of the limit viscosity (η_∞) as a function of volume

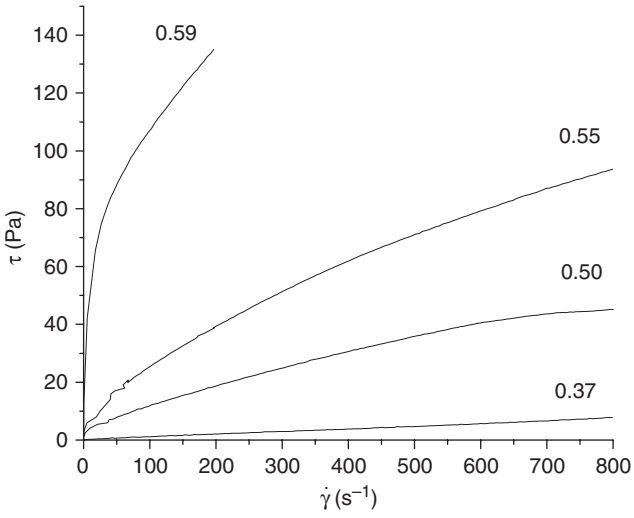

Fig. 5. Flow curves of aluminum oxide suspensions with different volume fractions measured in controlled shear mode (0.8 wt% polyelectrolyte and pH 10). Only up-curves are shown.

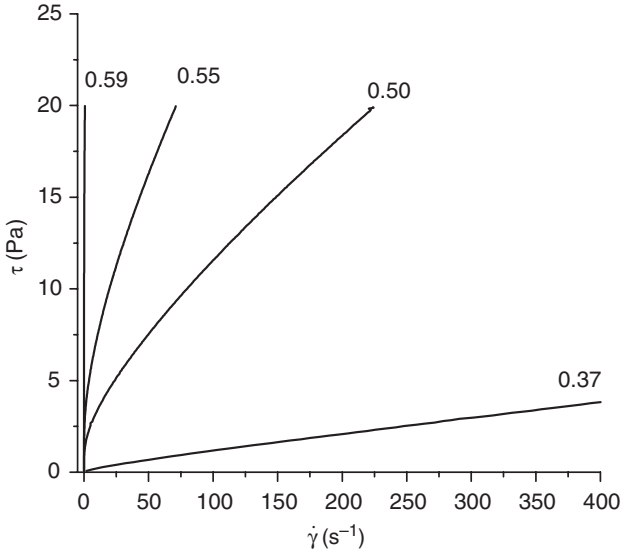

Fig. 6. Flow curves of aluminum oxide suspensions with different volume fractions measured in controlled stress mode (0.8 wt% polyelectrolyte and pH 10). Only up-curves are shown.

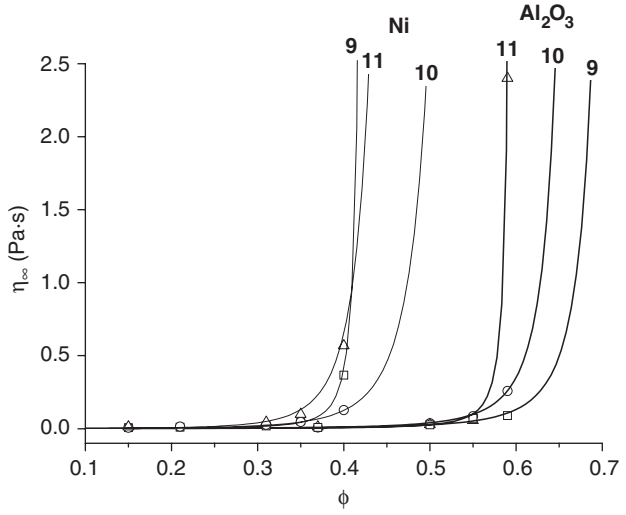

Fig. 7. Plot of the limit viscosity versus volume fraction of solids for nickel and aluminum oxide slurries. Curves represent the fitting to the Krieger–Dougherty model.

fraction of particles for Ni and alumina suspensions prepared at pH 9, 10, and 11.

Table I reports the values of n and ϕ_m for Ni and Al_2O_3 suspensions prepared at pH values of 9, 10, and 11 obtained by fitting the experimental data to the Krieger–Dougherty model Eq. (2). For monodisperse particles, the theoretical packing fraction is 0.72, and the values obtained here are not so far from the theoretical limit. A maximum packing fraction of 0.60

Table I. Parameters of Modified Krieger–Dougherty Fitting for Nickel (Ni) and Aluminum Oxide (Al_2O_3) at pH 9, 10, and 11

	Ni		Al_2O_3	
pH	*n*	ϕ_m	*n*	ϕ_m
9	2.3	0.42	3	0.74
10	4.5	0.60	3	0.70
11	4.0	0.50	1.9	0.60

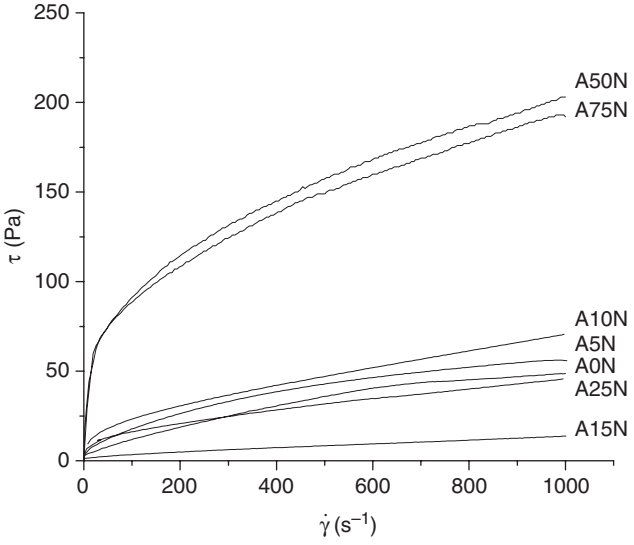

Fig. 8. Flow curves of aluminum oxide (Al_2O_3)—nickel (Ni) suspensions with different relative ratios of Ni measured in controlled shear mode (volume fraction of 0.5, 1 wt% polyelectrolyte, and pH 10). Only up-curves are shown.

is obtained for Ni at pH 10, but it decreases to 0.50 at pH 11 and to 0.42 at pH 9. The maximum packing fraction for alumina was very high (>0.60) at any pH, with a maximum of 0.74 for pH 9. The ϕ_m value decreases as pH increases, as a consequence of the higher viscosity.

(2) Rheological Behavior of Al_2O_3–Ni Mixtures

Once the dispersing conditions and the rheological behavior of pure Ni and pure Al_2O_3 suspensions were optimized, mixtures with concentrations of Ni ranging from 5 to 75 vol% were studied. Figure 8 shows the CR flow curves of all mixtures prepared to a volume fraction of solids of 0.50 at pH 10. For simplicity, only the up-curves have been plotted, but all mixtures exhibited a significant thixotropic cycle, which suggests the existence of a network structure that breaks on shearing. The addition of small concentrations of Ni (5 and 10 vol%) increases the viscosity as compared with that of pure alumina suspension. However, the addition of higher contents of Ni (15 and 25 vol%) leads to lower viscosity. This can be explained in terms of bimodality considering that Ni particles have an average size six times larger than that of alumina, thus allowing better packing of particles.[30] Suspensions with higher relative contents of Ni ($\geq$ 50%) show a much higher viscosity with a very shear thinning behavior, the rheology being controlled by the major phase.

When the extended flow curves of these suspensions are fitted to the Cross model, new extrapolated viscosities are obtained for shear rates close to zero and infinity. Table 2 summarizes the viscosity of the Al_2O_3–Ni suspensions with $\phi = 0.50$ and pH 10 measured at a shear rate of 100/s, the extrapolated values at zero and infinite shear rate and the thixotropy measured from controlled rate flow curves. The minimum viscosity is obtained for the suspension with 15 vol% Ni but it is more thixotropic than suspensions with a lower content of Ni. The large thixotropy and the strong differences in viscosity between the zero shear and the high shear regions suggest that a strong structure is formed at rest, especially when the Ni content increases.

The formation of a strong structure at rest or under low shear conditions can be visualized in Fig. 9, which plots the log–log curves of viscosity as a function of shear rate for two suspensions with different Ni contents. These curves were obtained by measuring under controlled stress conditions. In both cases, the viscosity decreases as shear rate increases until a given value where there is a range with a smaller rate of viscosity increase. After this region, the viscosity decreases again as the shear rate

Table II. Rheological Parameters of Aluminum Oxide (Al_2O_3)–Nickel (Ni) Suspensions with $\phi = 0.50$ and pH 10

	Ni (vol%)				
Parameter	5	10	15	25	50
η (100/s) (mPa · s)	140	167	34	160	900
η_0 (Pa · s)	322.1	313.7	36.2	1.4×10^6	4.2×10^6
η_∞ (mPa · s)	76.5	38.4	13.1	38.6	40.0
Thixotropy (Pa/s)	12320	8628	16990	55710	25100

increases. This region suggests that particles rearrange when some stress is introduced and that structure is broken before the particles start to flow. In the figure, the dotted lines correspond to fitting according to the Cross model. Considering the disruption of measured values in the CS curve, where no possible fitting can be obtained for the entire shear rate range, such that both shear zones were fitted independently. In this way, viscosity values could be extrapolated to zero and infinity for each suspension. The corresponding values of η_0 and η_∞ have been plotted as a function of the Ni content, as can be seen in Fig. 10. The values of η_0 were very low up to Ni contents of 15 vol%. Afterward, the viscosity grew exponentially with Ni content. In the case of η_∞, there is no clear tendency, the viscosity remaining roughly constant and independent of Ni content. This suggests that on shearing the suspensions easily flow easily and a high dispersion is achieved.

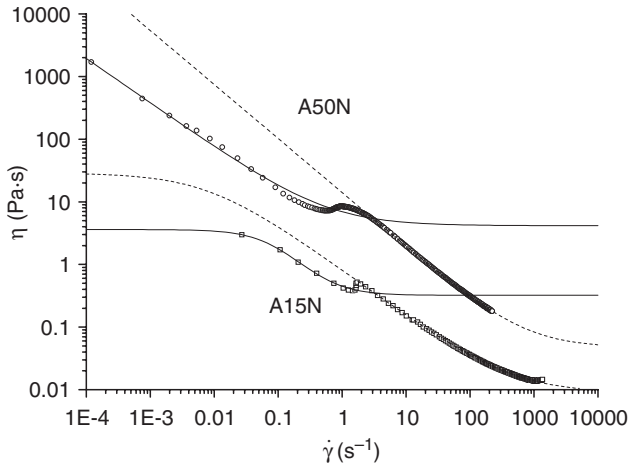

Fig. 9. Log–log plot for the aluminum oxide slurries with 15 vol% and 50 vol% of nickel. Only up-curves are shown. Lines indicate the fitting to the Cross model for the low shear region (solid lines) or the high shear region (dotted lines).

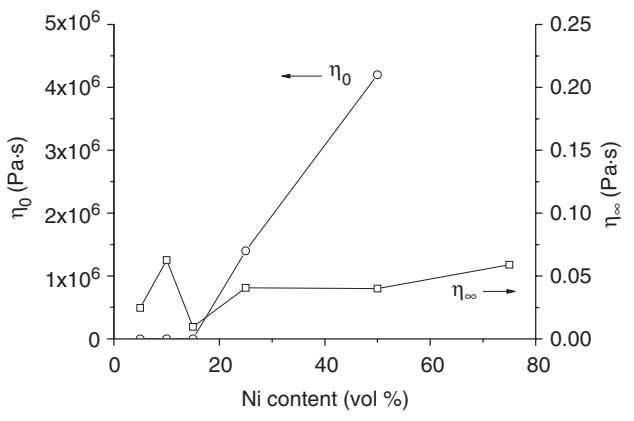

Fig. 10. Values of zero shear and limit viscosity versus nickel contents obtained after fitting the flow curves to the Cross model.

(3) Slip Casting Al_2O_3–Ni Composites

Al_2O_3–Ni suspensions with $\phi = 0.50$ and pH 10 were slip cast on plaster molds. Cast bodies were dried for 24 h under room conditions. The relative green densities of the samples are shown in Fig. 11. The relative green density of pure alumina cast pieces was 62% of the theoretical, and the relative density of mixtures increased for increasing concentration of Ni up to a maximum value of 72% of the theoretical for the mixture with 50 vol% Ni. This increment in the density is due to the bimodality of the powders used that allow a better packing of the particles during the consolidation of the green body.[10,31] However, the experimental data of mixtures with Ni contents higher than 50 vol% gave lower densities than expected. This is due to the high viscosity of concentrated suspensions (50 vol% solids) with Ni particles as the major phase. The large particle size of Ni powders and the high density of Ni make it difficult to prepare highly concentrated suspensions. Nevertheless, the mixtures prepared with 75 vol% Ni led to a relative density of the green bodies of 60% of TD, which is reasonably high.

Figure 12 shows the microstructure of green Al_2O_3–Ni cast bodies with Ni contents of 15 and 50 vol% obtained by SEM on fracture surfaces. It can be seen that the metal and alumina particles are uniformly co-dispersed.

Cast bodies were sintered in a flowing atmosphere of Ar with 1 vol% of O_2 at 1450°C/2 h in order to evaluate the microstructural uniformity and density. After sintering, samples had an outer oxidized layer composed of spinel and oxides (depending on the relative composition) that was ground off before any further measurement or treatment.[28] Figure 13 shows the SEM microstructure of polished sintered samples containing 10, 25, 50, and 75 vol% Ni. Pictures were obtained on polished surfaces without either thermal or chemical etching. The Ni phase appeared uniformly distributed into the alumina matrix and vice versa, and no agglomerates or large defects are observed in any of the samples obtained from the optimized suspensions. Figure 14 shows the SEM microstructure of sintered specimens with the largest content of Ni (50 and 75 vol%), after chemical etching. Uniform distribution of the minor ceramic phase can be also clearly seen in the etched samples. The sintered densities were

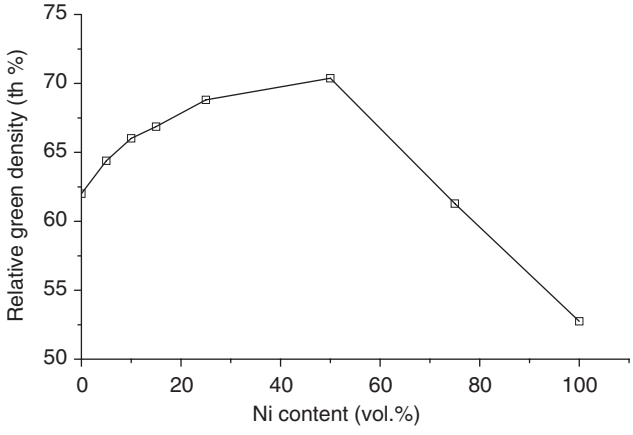

Fig. 11. Green density of slip-cast samples obtained from slurries with a total volume fraction of 0.50 and different nickel contents.

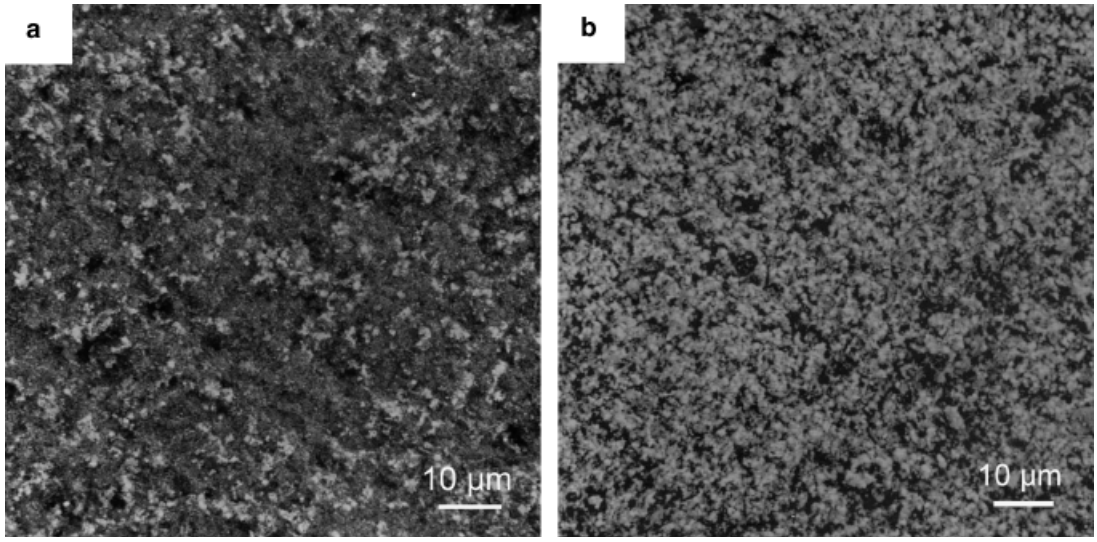

Fig. 12. Micrographs showing the fracture surfaces of green samples with nickel (Ni) contents of 15 (a) and 50 (b) vol% (Gray phase is Ni).

4.1, 4.3, 4.6, 5.0, 6.0, and 7.0 for samples with increasing contents of Ni from 5 to 75 vol%. Assuming that the sintered compacts do not react to form new species, the relative densities would be in the range of 97%–98% of the theoretical. The high density and the microstructural uniformity demonstrate that the slip casting process is suitable for manufacturing Al_2O_3–Ni composites if the complex colloidal and rheological behaviors are controlled.

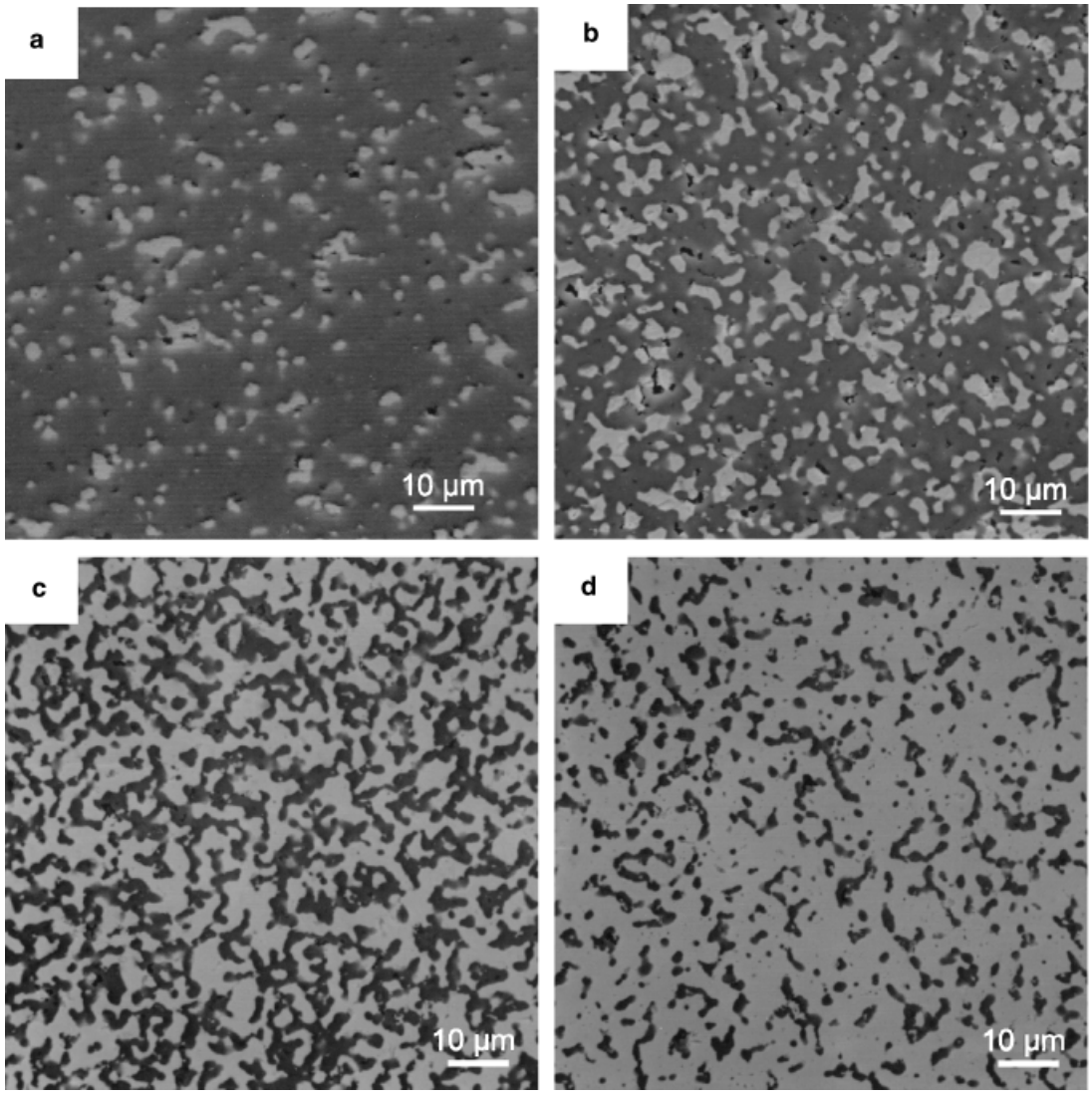

Fig. 13. Scanning electron microscopic microstructure of sintered samples with nickel (Ni) contents of 10, 25, 50, and 75 vol% (a, b, c, and d, respectively) (gray phase is Ni).

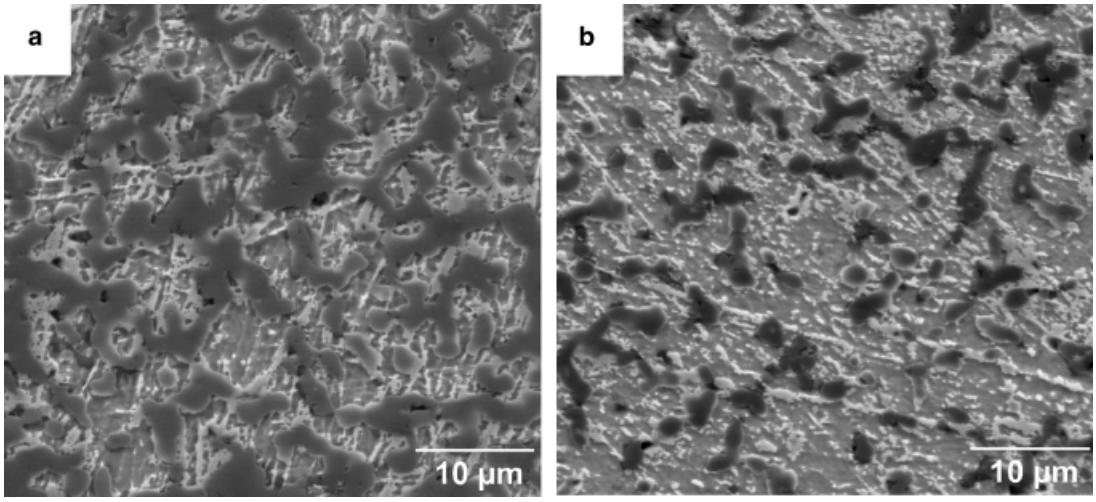

Fig. 14. Scanning electron microscopic microstructure of chemically etched samples with nickel (Ni) contents of 50 (a) and 75 vol% (b) (dark phase is Al_2O_3).

IV. Conclusions

The control of the surface behavior of Ni powders in water has allowed the preparation of concentrated suspensions of Al_2O_3–Ni mixtures, the best dispersing conditions being achieved for pH 10 with 1 wt% of an acrylic-based polyelectrolyte. The rheological behavior of mixtures with different relative contents of Ni and a total volume fraction of solids of 0.50 is strongly affected by the relative ratio of Ni and by its coarser particle size, which leads to sedimentation. The minimum viscosity, however, was found to occur for mixtures with 15 vol% Ni, which has been associated with a better packing of particles as a consequence of bimodality. Homogeneous pieces were obtained by slip casting suspensions with $\phi = 0.50$, leading to a maximum relative green density of 72% of TD for the mixture with 50 vol% Ni. The cast samples were sintered to 1450°C/2 h in an Ar atmosphere, leading to a high microstructural uniformity and relative sintered densities above 97% of TD.

References

[1]W. E. Windes, J. Zimmerman, and I. E. Reimanis, "Electrophoretic Deposition Applied to Thick Metal–Ceramic Coatings," *Surf. Coat. Technol.*, **157** [2–3] 267–73 (2002).
[2]S. F. Corbin and X. Qiao, "Development of Solid Oxide Fuel Cell Anodes Using Metal-Coated Pore-Forming Agents," *J. Am. Ceram. Soc.*, **86** [3] 401–6 (2003).
[3]W. H. Tuan and R. J. Brook, "Processing of Alumina/Nickel Composites," *J. Eur. Ceram. Soc.*, **10** [2] 95–100 (1992).
[4]X. D. Sun and J. Yeomans, "Optimization of a Ductile-Particle-Toughened Ceramic," *J. Am. Ceram. Soc.*, **79** [10] 2705–17 (1996).
[5]H. A. Bruck and B. H. Rabin, "Evaluating Microstructural and Damage Effects in Rule-of-Mixtures Predictions of the Mechanical Properties of Ni–Al_2O_3 Composites," *J. Mater. Sci.*, **34** [9] 2241–51 (1999).
[6]Y. Ji and J. A. Yeomans, "Microstructure and Mechanical Properties of Chromium and Chromium/Nickel Particulate Reinforced Alumina Ceramics," *J. Mater. Sci.*, **37** [24] 5229–36 (2002).
[7]G. Vekinis, E. Sofianopoulos, and W. J. Tomlinson, "Alumina Toughened with Short Nickel Fibres," *Acta Mater.*, **45** [11] 4651–61 (1997).
[8]T. Sekino, T. Nakajima, S. Ueda, and K. Niihara, "Reduction and Sintering of a Nickel-Dispersed-Alumina Composite and its Properties," *J. Am. Ceram. Soc.*, **80** [5] 1139–48 (1997).
[9]W. H. Tuan, H. H. Wu, and R. Z. Chen, "Effect of Sintering Atmosphere on the Mechanical Properties of Ni/Al_2O_3 Composites," *J. Eur. Ceram. Soc.*, **17** [5] 735–41 (1997).
[10]Z. C. Chen, K. Ikeda, T. Murakami, and T. Takeda, "Effect of Particle Packing on Extrusion Behavior of Pastes," *J. Mater. Sci.*, **35** [21] 5301–7 (2000).
[11]Z. Chen and J. J. Mecholsky, "Toughening by Metallic Lamina in Nickel Alumina Composites," *J. Am. Ceram. Soc.*, **76** [5] 1258–64 (1993).
[12]A. N. Winter, B. A. Corff, I. E. Reimanis, and B. H. Rabin, "Fabrication of Graded Nickel–Alumina Composites with a Thermal-Behavior-Matching Process," *J. Am. Ceram. Soc.*, **83** [9] 2147–54 (2000).
[13]F. F. Lange, "Powder Processing Science and Technology for Increased Reliability," *J. Am. Ceram. Soc.*, **72** [1] 3–15 (1989).
[14]J. A. Lewis, "Colloidal Processing of Ceramics," *J. Am. Ceram. Soc.*, **83** [10] 2341–59 (2000).
[15]J. Requena, R. Moreno, and J. S. Moya, "Alumina and Alumina Zirconia Multilayer Composites Obtained by Slip Casting," *J. Am. Ceram. Soc.*, **72** [8] 1511–3 (1989).
[16]J. S. Moya, A. J. Sanchez-Herencia, J. Requena, and R. Moreno, "Functionally Gradient Ceramics by Sequential Slip Casting," *Mater. Lett.*, **14** [5–6] 333–5 (1992).
[17]B. C. Weber, "The Application of the Slip Casting Process for the Forming of Cermets," *Interceram*, [1] 25–32 (1963).
[18]J. Chu, H. Ishibashi, K. Hayashi, H. Takebe, and K. Morinaga, "Slip Casting of Continuous Functionally Gradient Material," *J. Ceram. Soc. Jpn.*, **101** [7] 841–4 (1993).
[19]E. Antolini, M. Ferretti, and S. Gemme, "Preparation of Porous Nickel Electrodes for Molten Carbonate Fuel Cells by Non-Aqueous Tape Casting," *J. Mater. Sci.*, **31** [8] 2187–92 (1996).
[20]A. Y. Zaitsev, D. S. Wilkinson, G. C. Weatherly, and T. F. Stephenson, "The Preparation of Highly Porous Structures from Filamentary Nickel Powders," *J. Power Sources*, **123** [2] 253–60 (2003).
[21]W. J. Tseng and C. N. Chen, "Determination of Maximum Solids Concentration in Nickel Nanoparticle Suspensions," *J. Mater. Sci. Lett.*, **21** [5] 419–22 (2002).
[22]W. J. J. Tseng and C. N. Chen, "Effect of Polymeric Dispersant on Rheological Behavior of Nickel–Terpineol Suspensions," *Mat. Sci. Eng. A—Struct.*, **347** [1–2] 145–53 (2003).
[23]W. J. Tseng and S. Y. Lin, "Effect of Polymeric Surfactant on Flow Behaviors of Nickel–Ethanol–Isopropanol Suspensions," *Mat. Sci. Eng. A—Struct.*, **362** [1–2] 160–6 (2003).
[24]M. Y. Lin, H. M. Lindsay, D. A. Weitz, R. C. Ball, R. Klein, and P. Meakin, "Universality in Colloid Aggregation," *Nature*, **339** [6223] 360–2 (1989).
[25]N. Hernandez, R. Moreno, A. J. Sanchez-Herencia, and J. L. G. Fierro, "Surface Behavior of Nickel Powders in Aqueous Suspensions," *J. Phys. Chem. B*, **109** [10] 4470–4 (2005).
[26]N. Hernandez, A. J. Sanchez-Herencia, and R. Moreno, "Forming of Nickel Compacts by a Colloidal Filtration Route," *Acta Mater.*, **53** [4] 919–25 (2005).
[27]C. A. Gutiérrez and R. Moreno, "Interparticle Potentials of Aqueous Alumina Suspensions," *Br. Ceram. Trans.*, **102** [5] 219–24 (2003).
[28]K. P. Trumble and M. Ruhle, "The Thermodynamics of Spinel Interphase Formation at Diffusion-Bonded Ni/Al_2O_3 Interfaces," *Acta Metall. Mater.*, **39** [8] 1915–24 (1991).
[29]A. J. Sanchez-Herencia, N. Hernandez, and R. Moreno, "Fracture Behaviour of Pressureless Sintered Nickel-Reinforced Alumina Composites," *Key. Eng. Mater.*, **290**, 324–7 (2005).
[30]R. J. Farris, "Prediction of the Viscosity of Multimodal Suspensions from Unimodal Viscosity Data," *Trans. Soc. Rheo.*, **12** [2] 281–301 (1968).
[31]C. C. Furnas, "The Relations Between Specific Volume, Voids, and Size Compositions in Systems of Broken Solids of Mixes Sizes," *Bur. Mines Rep. Invest.*, **2894** [7] 1–10 (1928). □